Admittance Model Identification of Inverters using Voltage Injection

Original
Admittance Model Identification of Inverters using Voltage Injection / Zeppegno, L.; Mandrile, F.; Armando, E.; Bojoi, R.. - 2020-:(2020), pp. 2933-2938. ((Intervento presentato al convegno 46th Annual Conference of the IEEE Industrial Electronics Society, IECON 2020 tenutosi a Singapore (Singapore) nel 2020 [10.1109/IECON43393.2020.9254355].

Publisher:
IEEE Computer Society

Published
DOI:10.1109/IECON43393.2020.9254355

Admittance Model Identification of Inverters using Voltage Injection

Luca Zeppegno, Fabio Mandrile, Eric Armando and Radu Bojoi
Dipartimento Energia 'Galileo Ferraris'
Politecnico di Torino
Torino, Italy
zeppegno.luca@gmail.com, fabio.mandrile@polito.it, eric.armando@polito.it, radu.bojoi@polito.it

***Abstract*—The advancements in power electronics are leading to a growing number of electronic converters connected to the electric grid. Even though this enables a more efficient transformation and use of energy, the harmonic interaction between converters can cause instabilities in the network. Therefore, it is important to model the individual converters and their interconnection in an efficient way, in order to study the global stability of the system. A promising modelling strategy analytically derives the equivalent admittance of the converters. However, due to industrial secrecy issues, experimental identification methods are also necessary to obtain the converter equivalent admittance with a black-box approach. This paper analyses the experimental characterization of inverters using the voltage injection method. A detailed explanation of the theoretical background of this method and its practical implementation are provided.**

***Index Terms*—Admittance model, Stability analysis, Voltage injection**

I. INTRODUCTION

In the past few years the number of grid-tied electronic converters has greatly increased, mainly due to the increase of renewable energy sources (RES) and charging stations for electric vehicles (EVs). This growth is beneficial for the efficiency of the overall energy cycle, but it can also lead to harmonic interaction between converters that are connected to the same grid. This phenomenon is a system level issue, since the stability of the individual converters is ensured by their correct design. It is therefore important to further investigate such issues by developing accurate inverter models, which can predict the global stability of the network. This goal can be achieved by characterizing the electronic converter through a small-signal admittance model. These models can then be easily aggregated in order to obtain a global equivalent system, *e.g.* the one shown in Fig. 1. This overall system is used to asses the stability of the network by applying the Generalized Nyquist Criterion (GNC), as proved in [1], [2].

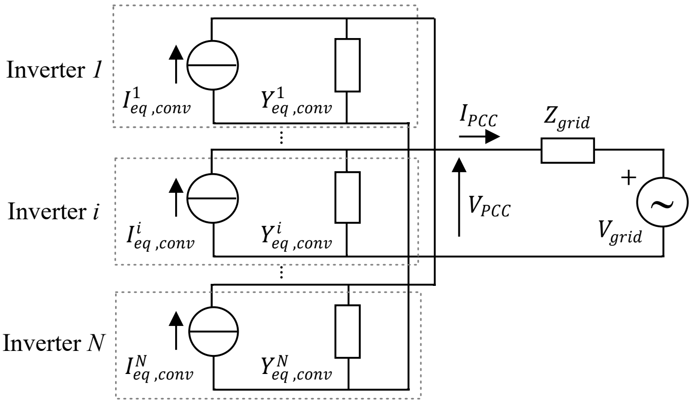

Fig. 1. Overall equivalent model of grid and converters.

A theoretical calculation of the converter admittance model is possible and applicable whereas the hardware and control details are known. However, this is usually not true for commercial solutions because of industrial secrecy issues. Therefore, identification methods to experimentally obtain the equivalent admittance model must be studied. These methods can be summarized as:

- Injection methods: with black-box [3]–[5] or grey-box approach [6]–[9]. These represent the most widespread solutions in technical literature.
- System Identification methods, where a step perturbation is generated on the output current and the voltage transient response is analysed in order to estimate a transfer function that, given the same step, would produce a similar output [10]–[12]. System Identification algorithms generally produce less reliable results than the injection methods.

This paper focuses on injection methods. Among these, the most common is the Current Injection Method (CIM), where a current generator is connected in parallel with an operating converter and injects a current at a test frequency. An alternative method is the Voltage Injection Method (VIM), where a voltage generator is connected in series with the converter and the grid, and is in charge of performing a voltage injection on the Point of Common Coupling (PCC). While technical literature expressed the possibility of using this method, information on describing an implementation on an experimental set-up are lacking. This is deeply studied in this paper in every aspect of its implementation.

The goal of this paper is therefore to provide a detailed explanation of the experimental characterization of inverters using the voltage injection method. Experimental results are then compared to theoretical results, which were calculated based on [13].

This paper is organized as follows. In Section II the theoretical background to this method is presented. In Section III the detailed step-by-step experimental method for voltage injection-based characterization is shown. Finally, Section IV presents the results of the experimental characterization and a comparison with the theoretical model.

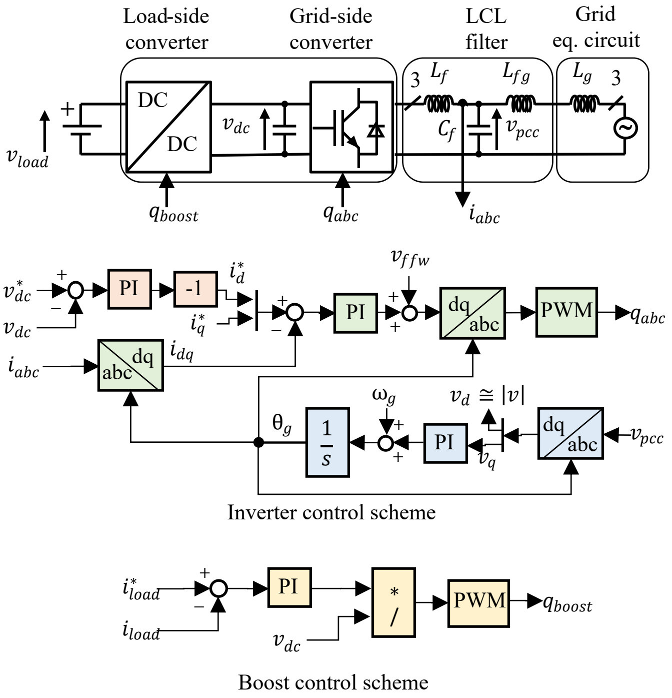

Fig. 2. Simplified diagram of the case under study, representing the electrical circuit and the control.

II. THEORETICAL BACKGROUND

The converter structure that was characterized in this paper is the one shown in Fig. 2. It is a two-stage AD/DC converter, composed by a DC/DC stage with an input current control and a AC/DC stage with DC voltage control and output current control in the (d, q) rotating reference frame. This frame is synchronous and coincident with the grid voltage vector, whose angle is observed through a Phase-Locked Loop (PLL). The switching frequency of the power modules is set at 10 kHz, while the bandwidth of the current control of both the AC/DC and DC/DC stages is 1 kHz. The DC-link voltage V_{dc} is controlled at 370 V through a voltage loop with 30 Hz bandwidth. Every control loop uses a proportional-integral (PI) regulator. Overall, this is a common structure for grid-tied converters such as active rectifiers and solar inverters. However, the characterization procedure that will be described is valid for every AC/DC topology and every control structure.

When considering experimentally-measured linear equivalent models of power converter, two considerations must be done:

- Since the converter is a non-linear system, it must be characterized at various operating points. This is an issue, since many power converters are designed to work at high power levels and this reflects on the operating points to be considered. Therefore, this usually precludes the possibility to use commercially available impedance analysers, which produce accurate results but cannot be used to characterize high power converters.
- Since only one measurement at a time is possible, every signal injection technique requires the system to work at steady state, so that sequential or simultaneous measurements would produce the same results. Moreover, it must be possible to repeat the measurements as many times as necessary, always retrieving the same results.

As already mentioned, the voltage injection method considers a series voltage generator at the converter PCC, which performs a frequency sweep by injecting voltage perturbations. A simplified circuit is shown in Fig. 3. The injected voltage frequencies should not be higher than the Nyquist frequency of the converter control. The converter, which is current controlled, will react to the voltage perturbation by trying to minimize its effect on the controlled currents. By measuring the perturbed voltages and currents at the PCC, the equivalent admittance at the perturbation frequency can be calculated.

This equivalent admittance is calculated in the (d, q) reference frame. An analytical approach is possible, and has been reported in [13]. Briefly, it is based on a Laplace domain block representation of the converter hardware

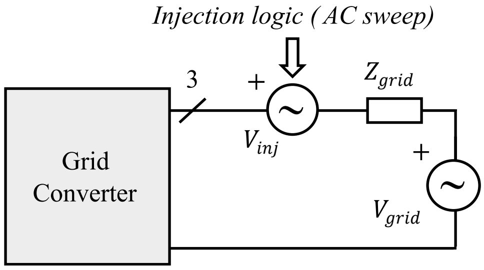

Fig. 3. Simplified representation of the voltage injection test circuit.

TABLE I. Converter values.

Grid electrical data		
Grid RMS phase voltage	$V_{g,RMS}$	120 V
Grid frequency	f_g	50 Hz
Output LC filter		
Output inductor	L_f	545 µH
Output capacitor	C_f	22 µF
DC-link		
DC-link capacitor	C_{DC}	1.8 mF
DC-link set point	$V_{DC,ref}$	370 V
DC/DC Converter		
DC/DC input inductor	L_{DC}	10 mH
Input DC voltage	V_{load}	300 V
Input DC voltage	I_{load}	8.5 A
Converter switching data		
ISR update frequency	f_{sw}	10 kHz

and control, where every block must be linearised around an operating point. It is therefore possible to obtain an overall transfer function representing the whole converter behaviour, which can link a small-signal grid voltage perturbations to the absorbed or injected current.

In order to measure the impedance matrix in the (d, q) rotating reference frame, two tests have to be considered with two linearly independent perturbation signals. The impedance matrix can then be calculated as shown in (1). The demonstration of this formula was already described [4] and will therefore not be explained in this paper.

$$\begin{bmatrix} Y_{dd} & Y_{dq} \\ Y_{qd} & Y_{qq} \end{bmatrix} = \begin{bmatrix} I_{d,1} & I_{d,2} \\ I_{q,1} & I_{q,2} \end{bmatrix} \cdot \begin{bmatrix} V_{d,1} & V_{d,2} \\ V_{q,1} & V_{q,2} \end{bmatrix}^{-1} \tag{1}$$

In (1), Z_{dd}, Z_{dq}, Z_{qd} and Z_{qq} are the terms of the impedance matrix, $V_{dq,1}$ and $V_{dq,2}$ are the (d, q) components for the first and second voltage injection and $I_{dq,1}$ and $I_{dq,2}$ are the (d, q) components of the current response.

There are many ways to obtain linearly independent signals. It is clear that only a change in the amplitude of the voltage perturbation is not sufficient, since the new perturbation would be linearly dependent. Some solutions, as in [4], use a phase shift in the voltage perturbation vector, while others [3] consider two different injections at the same frequency in the (d, q) frame, but corresponding to two different frequencies and sequences (positive and negative) in the stationary frame. The latter was applied in this paper. The two considered test frequencies are symmetric with respect to the perturbation frequency f_{inj} under study. In fact, if a perturbation frequency f_{dq} in the (d, q) frame is needed, it can be obtained with two different three phase signals:

- A positive sequence rotating in the three phase reference frame at $f_p = f_{inj} + f_r$:

$$V_{inj,1} = \hat{V}_{inj} \cdot \begin{bmatrix} cos(2\pi \cdot (f_{inj} + f_r) \cdot t) \\ cos(2\pi \cdot (f_{inj} + f_r) \cdot t - \frac{2\pi}{3}) \\ cos(2\pi \cdot (f_{inj} + f_r) \cdot t + \frac{2\pi}{3}) \end{bmatrix} \tag{2}$$

- A negative sequence rotating in the three phase reference frame at $f_n = f_{inj} - f_r$:

$$V_{inj,2} = \hat{V}_{inj} \cdot \begin{bmatrix} cos(2\pi \cdot (f_{inj} - f_r) \cdot t) \\ cos(2\pi \cdot (f_{inj} - f_r) \cdot t + \frac{2\pi}{3}) \\ cos(2\pi \cdot (f_{inj} - f_r) \cdot t - \frac{2\pi}{3}) \end{bmatrix} \tag{3}$$

where f_r is the voltage fundamental frequency. f_p and f_n are called *mirror frequencies* [3], since they are symmetrical and centred around the desired injected frequency $f_{d,q}$ in the (d, q) frame.

The impedance matrix described in (1) must be calculated at every frequency of interest f_{inj}. Therefore the final result will be a complex look-up table with the impedance at every analysed frequency.

A block diagram that summarizes the characterization procedure is shown in Fig. 4.

III. STEP-BY-STEP EXPERIMENTAL CHARACTERIZATION

The described procedure was validated on an experimental set-up, which is shown in Fig. 5. Its parameters are listed in Tab. I.

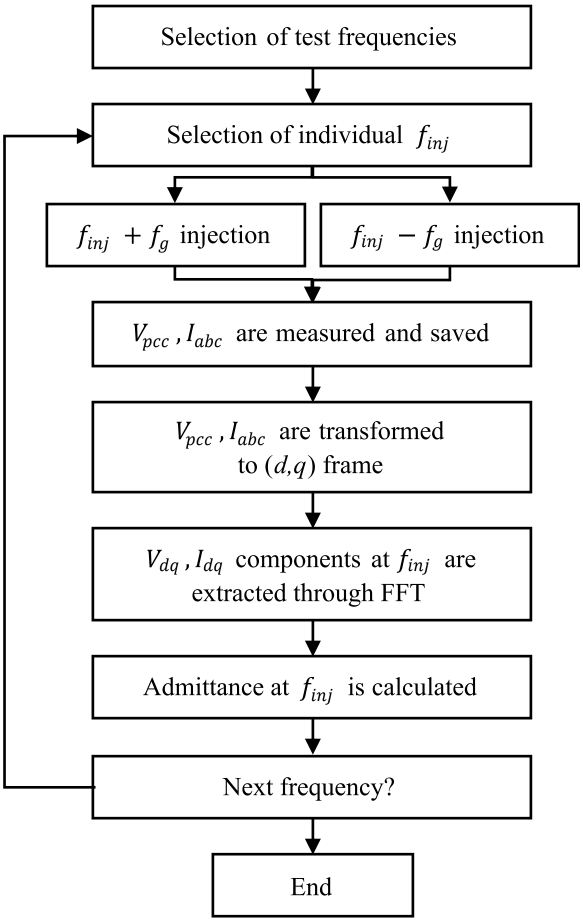

Fig. 4. Block diagram of the characterization procedure of the inverter.

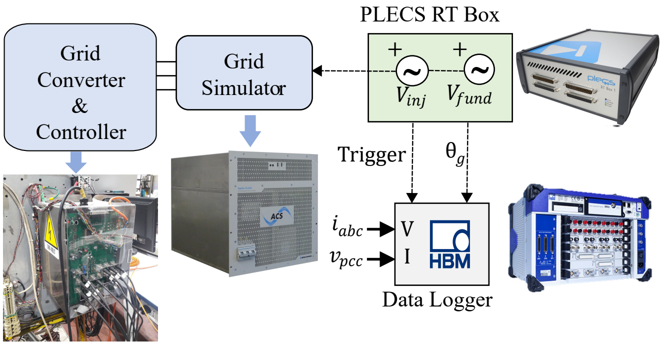

Fig. 5. Schematic of the experimental setup.

The injected voltage and the grid voltage were generated through a grid simulator, which was electrically connected to the converter. The simulator worked as an amplifier, with a source signal coming from a real-time simulator (*RT Box*) that can perform a *PLECS* simulation in real time and output selected values. The real-time simulator produced a reference voltage which was the sum of the grid fundamental voltage, set at 50 Hz and 120 Vrms, and the injected perturbation, with an amplitude of 0.1 p.u. and frequency dependant on the injection. The injection magnitude was therefore set at 12 Vrms in order to produce an observable current at high frequencies as well. It was also responsible of generating a trigger connected to data logger, in order to automatically start and stop the acquisitions when the injections were performed. The fundamental voltage angle was also extracted, in order to perform the transformation from the three phase to the rotating reference frame. The converter structure and control were the ones shown in Fig. 2, and the control was implemented on a dSPACE 1005.

Since many frequencies had to be tested, the procedure was automated. In order to do this, a list of test frequencies was generated. Therefore 50 logarithmically spaced frequencies f_{inj} from 10 to 1000 kHz were considered. The list was generated by the real-time simulator, which then considered one frequency at a time. Since the converter switching frequency is 10 kHz, the maximum test frequency is limited at 5 kHz. However, for this paper a lower maximum frequency had to be considered because of the grid simulator limits. Moreover, it must be highlighted that many of the most important frequencies in terms of stability are under 1 kHz.

For each frequency f_{inj}:

- A positive sequence three phase voltage was generated, first at the frequency $f_{inj} + f_r$. This perturbation was injected in the converter, and a start trigger was sent to the data acquisition system in order to start the measurement.
- The angle of the fundamental voltage was transferred from the real time generator, and saved by the data acquisition system. This angle is necessary to perform the transformation from the three phase frame to the rotating frame. In fact, it would be difficult to compute the angle directly from measured voltages because of the overlapped perturbation signal, which can be at a lower frequency than the fundamental one or at a higher one. Therefore a filtering with simple low pass filters and high pass filters would not be suitable in order to isolate the fundamental frequency. Since perturbations can also be around the fundamental frequency, even resonant filters are not ideal. It is not possible to use the angle observed by the converter PLL as it would introduce an error due to the reflect the loop dynamics dynamics. Therefore, exporting the correct angle from the real-time simulator had proven to be the most simple yet most effective

solution.

- After 20 electrical periods of the injected signal, the acquisition was stopped by a stop trigger generated by the real-time simulator. The minimum time for the acquisition was set at 1 second. This ensures the steady state operation of the converter, and only the last 10 electrical periods were then considered for the subsequent analysis.
- This process was repeated for a negative sequence voltage as well, at the frequency $f_{inj} - f_r$.

When the power frequency sweep was completed, the measurements were post-processed in MATLAB in order to calculate the admittances. For each frequency the following steps were accomplished at first for the positive sequence measurement, then for the negative sequence one:

- A filtering with a 10 kHz low-pass filter was applied in order to reduce measurement noise. The filtering was chosen in order to be the highest possible without affecting the measurements at the maximum frequency under test, which is 1000 Hz.
- The measurements were transformed into the fundamental (d, q) rotating frame, using the information on the fundamental angle.
- An FFT was applied in order to extract the amplitude and phase components at each considered test frequency f_{inj}.

The equivalent impedance was then calculated as shown in Eq. (1). This procedure was repeated for every frequency. The result of this process is shown in Section IV.

IV. Experimental Results

The results that were obtained with the procedure described in Section III are shown in Fig. 6. In order to perform the measurements, the converter operated as an active rectifier. The current that was absorbed from the grid was set at 10 A, while no reactive power was generated or absorbed ($i_d^* = 10A, i_q^* = 0A$).

The following comments can be done:

- A good agreement between theoretical and measured self-admittances is reported.
- As for the mutual admittances, there is a difference at low frequencies. The higher the frequency, smaller is this error. This issue is mainly due to measurement errors. In fact, the harmonic components that must be measured at low frequencies have an extremely low amplitude (<1A), and were measured with 200 A full scale hall effect sensors.

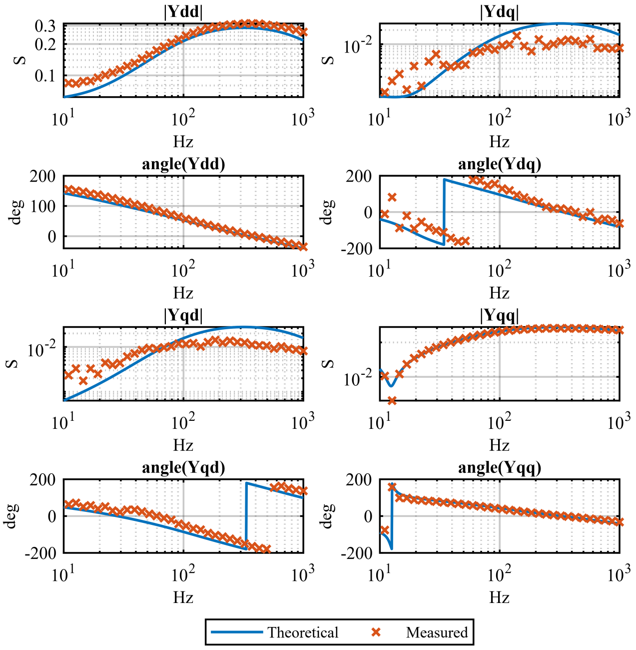

Fig. 6. Experimental results of the voltage injection method ($i_d^* = 10A, i_q^* = 0A$).

It must be noted that low scales sensors cannot be used because of the converter high power operating point. Since the admittances are small, a little error in the measurement can cause a great error in the calculated admittance. However, it must be pointed out that instability problems are more likely to occur in the proximity of the bandwidth frequency of the current control, which is much higher than the low frequency region where there is higher uncertainty on the result. Therefore this uncertainty is not a relevant problematic.

- The disturbance on the theoretical result at around 100 Hz is an issue that comes from the inversion of matrices which is required for the analytical calculation, and should not be considered.
- Some differences depend on the fact that the theoretical results were calculated considering an ideal DC/DC converter. Therefore they do not take into account the DC/DC non-idealities.

V. Conclusions

This paper presented a detailed experimental implementation of a grid inverter characterization through the voltage injection method. Although this method had been already introduced through an theoretical approach in the literature, there were lacking informations on its experimental implementation. Therefore, this paper presented a theoretical background on the functioning of the method and an experimental step-by-step procedure in order to implement it on a grid-tied converter. The results were then shown and compared with a theoretical solution.

The obtained results are reliable at high frequencies, while there is a major uncertainty at low frequencies.

As an advantage, this method can be performed automatically without the interaction of the user. Therefore, in an industrial environment, almost no previous knowledge or training is required to the testing engineer in order to perform this test. Moreover, the data processing is relatively simple and can be implemented on every programming language, thus a MATLAB license is not mandatory in order to perform this test.

As a conclusion, it can be stated that the voltage injection method appears to be a mature procedure that can be applied to the converter under test with low effort, when a grid simulator is available.

REFERENCES

[1] J. Sun, "Impedance-Based Stability Criterion for Grid-Connected Inverters," *IEEE Transactions on Power Electronics*, vol. 26, pp. 3075–3078, Nov. 2011.

[2] B. Wen, D. Boroyevich, R. Burgos, P. Mattavelli, and Z. Shen, "Inverse Nyquist Stability Criterion for Grid-Tied Inverters," *IEEE Transactions on Power Electronics*, vol. 32, pp. 1548–1556, Feb. 2017.

[3] A. Rygg, M. Molinas, C. Zhang, and X. Cai, "A Modified Sequence-Domain Impedance Definition and Its Equivalence to the dq-Domain Impedance Definition for the Stability Analysis of AC Power Electronic Systems," *IEEE Journal of Emerging and Selected Topics in Power Electronics*, vol. 4, pp. 1383–1396, Dec. 2016.

[4] G. Francis, R. Burgos, D. Boroyevich, F. Wang, and K. Karimi, "An algorithm and implementation system for measuring impedance in the D-Q domain," in *2011 IEEE Energy Conversion Congress and Exposition*, pp. 3221–3228, Sept. 2011.

[5] W. Liu, X. Xie, X. Zhang, and X. Li, "Frequency-coupling Admittance Modeling of Converter-Based Wind Turbine Generators and the Control-Hardware-in-the-Loop Validation," *IEEE Transactions on Energy Conversion*, pp. 1–1, 2019.

[6] M. Amin and M. Molinas, "A Gray-Box Method for Stability and Controller Parameter Estimation in HVDC-Connected Wind Farms Based on Nonparametric Impedance," *IEEE Transactions on Industrial Electronics*, vol. 66, pp. 1872–1882, Mar. 2019.

[7] W. Zhou, Y. Wang, and Z. Chen, "A Gray-Box Parameters Identification Method of Voltage Source Converter Using Vector Fitting Algorithm," in *2019 10th International Conference on Power Electronics and ECCE Asia (ICPE 2019 - ECCE Asia)*, pp. 2948–2955, May 2019.

[8] Z. Liu, H. Wu, W. Jin, B. Xu, Y. Ji, and M. Wu, "Two-step method for identifying photovoltaic grid-connected inverter controller parameters based on the adaptive differential evolution algorithm," *Transmission Distribution IET Generation*, vol. 11, no. 17, pp. 4282–4290, 2017.

[9] A. Riccobono, M. Mirz, and A. Monti, "Noninvasive Online Parametric Identification of Three-Phase AC Power Impedances to Assess the Stability of Grid-Tied Power Electronic Inverters in LV Networks," *IEEE Journal of Emerging and Selected Topics in Power Electronics*, vol. 6, pp. 629–647, June 2018.

[10] V. Valdivia, A. Barrado, A. LÁzaro, P. Zumel, C. Raga, and C. FernÁndez, "Simple Modeling and Identification Procedures for "Black-Box" Behavioral Modeling of Power Converters Based on Transient Response Analysis," *IEEE Transactions on Power Electronics*, vol. 24, pp. 2776–2790, Dec. 2009.

[11] V. Valdivia, A. Lázaro, A. Barrado, P. Zumel, C. Fernández, and M. Sanz, "Impedance Identification Procedure of Three-Phase Balanced Voltage Source Inverters Based on Transient Response Measurements," *IEEE Transactions on Power Electronics*, vol. 26, pp. 3810–3816, Dec. 2011.

[12] S. Neshvad, S. Chatzinotas, and J. Sachau, "Wideband Identification of Power Network Parameters Using Pseudo-Random Binary Sequences on Power Inverters," *IEEE Transactions on Smart Grid*, vol. 6, pp. 2293–2301, Sept. 2015.

[13] B. Wen, D. Dong, D. Boroyevich, R. Burgos, P. Mattavelli, and Z. Shen, "Impedance-Based Analysis of Grid-Synchronization Stability for Three-Phase Paralleled Converters," *IEEE Transactions on Power Electronics*, vol. 31, pp. 26–38, Jan. 2016.